Review Article

Myocardial Tissue Characterization by Cardiac Magnetic Resonance: A Primer for the Clinician

Suraj Gowda, Richa Jayesh Kothari, Vimal Raj

Cardiothoracic Imaging Unit, Department of Radiology, Narayana Institute of Cardiac Sciences, Narayana Hrudayalaya, Bengaluru, Karnataka, India

Abstract

Imaging plays an important role in the diagnosis, management, and prognosis of cardiac conditions. Over the last three decades, cardiac magnetic resonance (CMR) has established itself as a promising imaging tool in the assessment of patients with various cardiac ailments. CMR is now being considered as a one-stop-shop diagnostic test because of its ability to comprehensively assess the heart. The greatest strength of CMR is its ability to characterize the myocardium noninvasively aiding in the diagnosis of patients. Despite its growing use worldwide, the adoption of the modality in India has been relatively slow. One major reason for this is the lack of expertise and resources to perform CMR. Another reason for the slow adoption of CMR in India is the limited understanding of practicing clinicians on how the modality works and what the various clinical applications of CMR are. In this review, we aimed to address these shortcomings by outlining some basics of CMR and its utility in day-to-day practice with a special focus on myocardial tissue characterization.

Keywords: Cardiac magnetic resonance imaging, cardiomyopathy, myocardial tissue characterization

Introduction

Imaging plays an important role in the diagnosis, management, and prognosis of cardiac conditions. Over the last three decades, cardiac magnetic resonance (CMR) has established itself as a promising imaging tool in the assessment of patients with various cardiac ailments. CMR is now being considered as a one-stop-shop diagnostic test because of its ability to comprehensively assess the heart. CMR can provide both anatomical and functional data relating to the heart in a single examination and is not restricted by patients' body habitus or availability of suitable imaging windows. However, the greatest strength of CMR is its ability to characterize the myocardial morphology noninvasively, thus aiding in the accurate diagnosis of patients.

Echocardiography remains the first imaging modality of choice in the assessment of cardiac patients. Its universal availability, cost-effectiveness, and lack of exposure to radiation make it a unique imaging modality. CMR, on the other hand, requires high-end equipment and reporting expertise which is not easily available in all parts of the country. This has led to the slow adoption of the modality in routine clinical practice. Many clinicians are also not well versed with the functioning of CMR and its utility in day-to-day practice. In this review, we aimed to address these shortcomings by outlining some basics of CMR and its utility in day-to-day practice with a special focus on myocardial tissue characterization.

Basics of Cardiac Magnetic Resonance Imaging

Magnetic resonance imaging (MRI) works on the principles of nuclear magnetic resonance. By this, hydrogen atoms in the body when placed in an external magnetic field (the MRI machine) act as mini-magnets themselves. These mini-magnets can then be manipulated by applying different radiofrequency/gradient pulses to obtain an image. These pulses are the main reason for the noise inside the MRI scanner. MRI offers excellent soft-tissue resolution as hydrogen atoms are available in abundance within the body. The signal intensity

Address for correspondence: Dr. Vimal Raj, Cardiothoracic Imaging Unit, Narayana Institute of Cardiac Sciences, Narayana Hrudayalaya, Bengaluru - 560 099, Karnataka, India.
E-mail: drvimalraj@gmail.com

Submitted: 04-Sep-2022 **Accepted in Revised Form:** 24-Sep-2022
Published: 04-Jan-2023

How to cite this article: Gowda S, Kothari RJ, Raj V. Myocardial tissue characterization by cardiac magnetic resonance: A primer for the clinician. J Indian Acad Echocardiogr Cardiovasc Imaging 2023;7:16-30.

Access this article online

Quick Response Code:

Website: www.jiaecho.org

DOI: 10.4103/jiae.jiae_44_22

of tissue depends on the physical and chemical properties intrinsic to the tissue of interest and allows in differentiating various pathologies.[1]

CMR can be performed in MRI machines with a magnetic strength of 1.5 Tesla or more. The 3 Tesla machines are relatively faster and give better resolution, but can be prone to significant artifacts due to inherent infield inhomogeneities. Electrocardiogram (ECG) gating is essential and a good tracing is required to get better quality images. A clean skin surface helps in proper contact between skin and the ECG electrodes. Patients will be in a supine position with the arms by the side of the torso. A coil (flat board like material) is placed on the chest for acquiring the images. The scan usually lasts for 30–45 min and the patients are given breath-hold instructions and often asked to practice this prior to the appointment. Imaging can also be performed in a "free breathing" status in patients who cannot hold their breath. Myocardial evaluation ideally requires the use of intravenous gadolinium-based contrast media. These are safe in most patients with maintained renal function.

CMR is a very safe modality and does not use ionizing radiation. Noise-reducing headphones are used to reduce the discomfort caused by the loud noise of the scanner and to communicate with the patient. Newer advances with a wider bore of the scanner and visual aids (ability to watch a television inside the gantry) help in calming patients with claustrophobia. General MRI precautions relating to metallic objects and implants are taken as standard. Patients with MRI compatible cardiac implantable electronic devices can also undergo a CMR examination after consultation and review by the electrophysiology team.[2]

Cardiac Magnetic Resonance Protocols

Images acquired during a CMR examination can be broadly classified into 4 groups based on their utility: anatomical, functional, morphology, and phase contrast flow.

Anatomy

Multiplanar and 3-dimensional images are easily obtained with CMR without the use of a contrast agent. This is extremely useful in the assessment of patients with congenital heart diseases (CHD) and those with vascular anomalies. CMR is not limited by patients' body habitus or dependent on the availability of imaging windows. Images can be obtained either during breath-hold or while breathing freely. Contrast-enhanced or noncontrast angiography studies are also possible for accurate assessment of the vascular anatomy.

Functional assessment

CMR is considered the gold standard in the assessment of ventricular function.[3] It is a highly reproducible test with good interobserver concurrence. Functional CMR or cine CMR routinely uses cine steady-state-free-precession sequences, which is a fast and robust technique that offers good contrast resolution between the blood and the myocardium [Figure 1]. Complete volumetric data of the ventricles are acquired and analyzed using dedicated software to get accurate ventricular volumes, cardiac output, and ejection fractions. Any ventricular morphology (i.e. normal/dilated or aneurysm) will not alter the accuracy of the functional assessment on CMR. Artificial intelligence/machine learning algorithms have made this quantification very fast and robust.

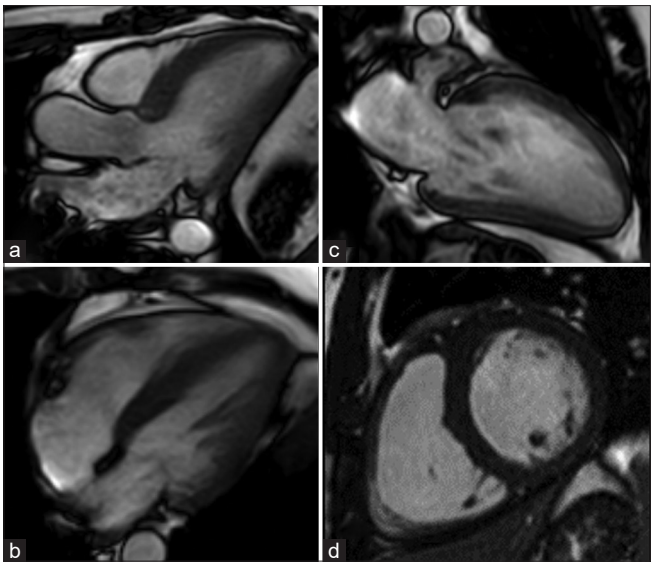

Figure 1: Functional assessment using steady-state-free-precession images in different imaging planes. A three-chamber (a) four-chamber (b) two-chamber (c) and short-axis (d) images of a patient being evaluated for coronary artery disease

Strain imaging

Myocardial deformation imaging using CMR is growing in use for the early detection of ventricular contractile dysfunction. Myocardial strain is a measure of the extent of deformation of a segment of the myocardium from its initial dimension [Figure 2]. With CMR, it is possible to evaluate longitudinal, circumferential, and radial strain in a given patient. Many acquisition methods for the evaluation of myocardial strain have been described, including CMR tagging, phase velocity mapping, displacement encoding with stimulated echoes, and strain-encoded imaging.[4-7] CMR can also assess right ventricular (RV) strain patterns.[8,9] Preliminary results on atrial strain assessment by CMR also seem to be promising.[10,11] Myocardial strain is of prognostic importance, even when systolic function and other morphological parameters, such as late gadolinium enhancement (LGE), are normal. The impaired myocardial strain has also been shown to predict major adverse cardiac events.[11]

Morphology

CMR has the unique ability to assess myocardial tissue character and differentiate one pathology from the other. This is achieved using a combination of different imaging sequences.

Edema

Short tau inversion recovery (STIR) sequence is used to assess for myocardial edema. These images are acquired in breath-hold and can be taken in any imaging plane of choice. This sequence is highly sensitive for water and the timing of the sequence is

such that the signal from fat and the blood within the ventricular cavity is suppressed (triple inversion recovery).[12] These images help in discrimination between acute and chronic ischemic myocardial injury, identification of foci of myocarditis, and inflammatory foci in nonischemic inflammatory/infective cardiomyopathies. It also helps in the early noninvasive detection of acute organ rejection.

Myocardial mapping

Parametric mapping is a novel biomarker that provides deeper insight into the myocardial properties and supports diagnostic, therapeutic, and prognostic decision-making in ischemic and nonischemic cardiomyopathies.[13] Quantitative mapping of T1, T2, and T2* (T2 star) characteristics allows noninvasive myocardial tissue characterization without using intravenous contrast agents.[14]

T1 mapping

Every tissue in the body has a unique T1 time, which varies with different pathology. T1 time is defined as the time needed for the protons to re-equilibrate after being excited by a radiofrequency pulse. Parametric maps are generated during breath-hold in a specific imaging plane. T1 map refers to pixel-wise demonstration of absolute T1 time on a map which is often color coded [Figure 3]. This value is dependent on the magnetic field strength (1.5 vs. 3T), type of tissue being examined, and whether contrast media is used or not.[15] These parametric maps have a higher sensitivity to myocardial alterations and can highlight minor variations in T1, which is otherwise inapparent in other noninvasive means. Native T1 (without contrast) values get prolonged due to expansion of the interstitial space secondary to deposition of water (edema), amyloid protein, or fibrosis/scar tissue. On the other hand, there is a reduction in T1 values in patients with deposition of iron or lipid (Anderson–Fabry disease).

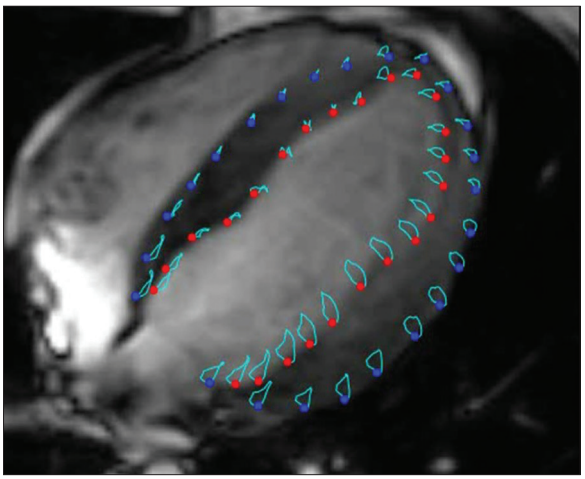

Figure 2: Representation of cardiac magnetic resonance strain assessment using feature tracking in a 4-chamber plane

Contrast-enhanced T1 and extracellular volume

Another important component of T1 mapping is the estimation of extracellular volume (ECV) by analysis of native (precontrast) and contrast-enhanced T1 myocardial maps, using blood hematocrit as a reference for the T1 changes within the myocardium. This essentially correlates the change of T1 values of the myocardium to that of blood. ECV measurement can be of importance in conditions where there is diffuse interstitial remodeling and expansion (for example, myocarditis, myocardial infarction, and dilated cardiomyopathy [DCM]).[16] In short, native T1 is a reflection of both intracellular and extracellular compartments, while the ECV is a reflection of the extracellular compartment [Figure 3].[17]

T2 mapping

T2 time is the time needed for decay in magnetization along the transverse vector. Similar to T1 mapping, parametric T2 maps can be generated through multiple image acquisition at different T2 times. In comparison to T1 values, the normal myocardial T2 values tend to have a wide range of variability between subjects.[18] The difference in T2 values between normal and diseased myocardium is very small.[19] The major utility of T2 mapping is in the detection of myocardial edema in numerous pathologies, including acute infarction, myocarditis, and transplant rejection.

T2* mapping

T2 star (or T2*) mapping is primarily used to detect iron content in the liver and myocardium. A 1.5T MRI scanner is preferred as 3T scanners tend to produce more artifacts if the iron content is very high (due to increasing magnetic field inhomogeneities at higher field strengths). The normal values are dependent on the magnetic field strength of the MRI

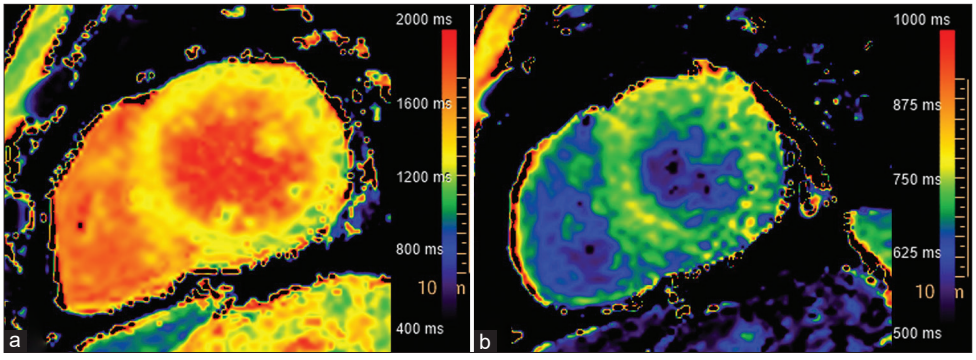

Figure 3: Normal native T1 mapping (a) and extracellular volume (b) images in short-axis

scanner and the cutoff for tissue iron overload is generally lower at higher field strength. Normal ranges for myocardial and liver iron concentration are available and can be used for the assessment of disease severity and monitoring response to chelation therapy. In addition, T2* mapping has also been used to detect myocardial ischemia due to coronary artery disease, for the assessment of endothelial function and to distinguish between focal and diffuse fibrosis.[20-22]

Postcontrast imaging

Gadolinium based contrast agents (GBCA) have been used in CMR for the last two decades as a leading method for myocardial tissue characterization. Gadolinium is a paramagnetic contrast agent and is administered intravenously in CMR. It leads to shortening of both T1 and T2 times with increased brightness on T1 and the opposite on T2 weighted images. Gadolinium leads to enhancement of the intravascular compartment and the interstitium. The former is useful in anatomical assessment of the vasculature and the latter is instrumental in myocardial tissue characterization. Safety profile of GBCAs is very good, especially in patients with good renal function. There is an association of nephrogenic systemic fibrosis in renal failure patients receiving GBCA. There is recent consensus which supports the use of specific types of GBCA (group 2) even in patients with poor renal function (glomerular filtration rate <30) irrespective of dialysis status.[23,24]

Early gadolinium enhancement

Early gadolinium enhancement (EGE) images are acquired soon after administering a GBCA. EGE assesses capillary leakage and microcirculatory disturbance. It is especially useful to identify microvascular obstruction, intracavitary thrombus, and for the assessment of acute myocarditis.[25] It has also been used as a potential marker of the disease burden in hypertrophic cardiomyopathy (HCM).[26]

Late gadolinium enhancement

LGE imaging is typically performed about 7–10 min after giving the GBCA. This gives enough time for the gadolinium to accumulate in the interstitial tissue and become easily detectable. The CMR sequence is performed in such a manner that the normal myocardium is black in color (nulled) and abnormal tissue is white/bright in signal. Imaging is usually performed in short-axis, 2-chamber and 4-chamber planes with the acquisition of data in a volumetric manner so the amount of enhancement can be accurately quantified. LGE is unparalleled in myocardial tissue characterization and has provided significant prognostic benefits in various conditions. The pattern and extent of LGE allow to differentiate one pathology from another and also help in monitoring the progression of the disease.

T1 and T2 spin-echo sequences

These are standard MRI sequences that help in the characterization of tissue based on the proton density and tissue structure. These do not provide functional information and usually take a longer time to acquire. These are largely replaced by mapping sequences for myocardial assessment and are reserved for the assessment of tumors and extra cardiac lesions in CMR. The blood pool within the Left ventricular (LV) cavity is mostly dark in these sequences and provides good contrast differentiation from the adjoining myocardium.

Phase-contrast velocity mapping

Phase-contrast CMR (PC-CMR) technique is very similar to the Doppler technique used in echocardiography. In this technique, we can accurately assess the direction of blood flow and quantify it. Compared to Doppler, PC-CMR can be acquired in any imaging plane and has a much higher spatial resolution. PC-CMR obtains two image sets, a magnitude image (anatomical image where signal intensities correspond to the tissue properties) and a phase image (where signal intensities correspond to the blood flow velocity). Data are typically obtained over multiple cardiac cycles with the use of ECG gating and can be obtained either during breath-hold or free-breathing (more physiological). Velocity encoding (VENC) is a parameter that needs to be specified before performing this sequence. VENC is measured in cm/s and relates to the highest velocities that are likely to be seen in the vessel that is being imaged. PC studies are routinely used for assessment/quantification of valvular diseases, both for stenosis and regurgitation. It is also accurate in the assessment of shunts and quantify its severity, i.e. the Qp: Qs. Newer advances in PC imaging (4-dimensional Flow) allow the acquisition of a large multidimensional dataset that provides functional and flow data together and can be manipulated in any imaging plane for postprocessing.

Common Applications of Cardiac Magnetic Resonance in Day-to-Day Practice

Ischemic heart disease

Cardiac MRI is becoming an invaluable imaging modality in assessment of selected patients with ischemic heart disease. CMR provides a comprehensive assessment of patients by accurate quantification of ventricular function, myocardial perfusion, and delineation of infarcted/ischemic segments from the normal ones. Two clinical scenarios commonly encountered are assessment of myocardial ischemia and/or myocardial viability.

Myocardial ischemia

Ischemia assessment on CMR can be performed either by first pass perfusion analysis using adenosine or by assessment of inducible wall motion abnormality using dobutamine. These agents are safe in the CMR environment and give reliable results.[27-30] Dobutamine stress is performed on similar lines to those of echocardiography and areas of new regional wall motion abnormality are detected during increasing stress. With adenosine, contrast is injected during peak stress and the perfusion of the myocardial segments is directly visualized. The same is repeated during rest (about 7–10 min after stress imaging) to assess for areas of fixed perfusion defect (infarction) and reversible perfusion defect (inducible ischemia) [Figure 4].

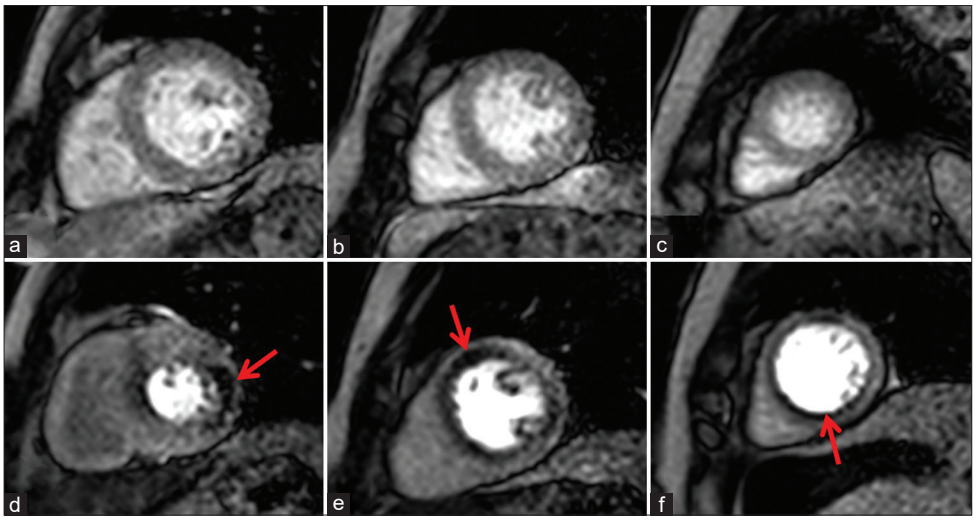

Figure 4: Myocardial ischemia assessment. Short-axis images in basal, mid and apical levels (a-c) during rest and the corresponding images at peak stress (d-f). Areas of reduced perfusion/perfusion defects (red arrows) are seen in the stress images in keeping with reversible perfusion defects

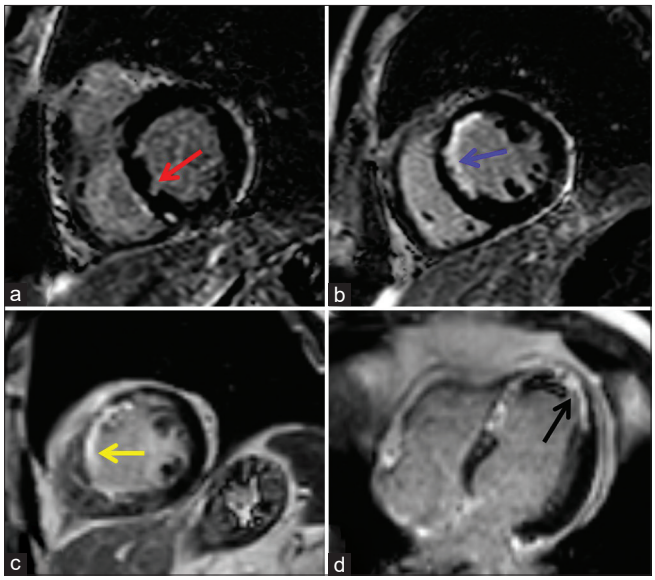

Figure 5: Late gadolinium enhancement images of different patients with varying degrees of infarction. (a) Subendocardial infarct (red arrow) (b) Intermediate infarct (blue arrow) (c) Near transmural infarct (yellow arrow) (d) Transmural infarct (black arrow)

Myocardial viability

Cardiac MRI is excellent in recognizing viable/hibernating tissue which would benefit from revascularization. In CMR, viability can be assessed by various measures including myocardial wall thickness/wall motion, LGE and low-dose dobutamine MRI.[31]

LGE images clearly differentiate areas of infarction (bright) from normal tissue (black). Typically, infarction tends to occur in the subendocardial region of myocardium and progresses toward the epicardium. The infarction is thus categorized as subendocardial (<25% of myocardial thickness involvement), intermediate (25%–50% of myocardial thickness involvement), near transmural (50%–75% of myocardial thickness involvement), and transmural if more than 75% of myocardial thickness is involved [Figure 5]. In patients with 50%–75% thickness infarction, contractile improvement can be expected in 10% of cases while in those with >75% of infarction the contractile recovery can be expected in <1% of cases.[32] On LGE, it is important to differentiate myocardial infarction from other causes of myocardial enhancement (such as inflammation or infiltration). Noninfarct related enhancement typically involves midmyocardium or the epicardium and are in a nonvascular territory. LGE assessment for viability can overestimate the extent of infarction in patients with acute myocardial infarction wherein areas of myocardial edema (peri-infarct territory) will also show LGE.

Progressive thinning of myocardium is seen with chronic infarction. End-diastolic wall thickness of <5.5 mm has been shown as a sensitive marker to predict nonrecovery post-revascularization.[33] This also can be used as a marker of viability on CMR in patients who cannot undergo the complete assessment or cannot be given GBCA due to renal dysfunction or allergy.

The use of low-dose dobutamine is reserved for patients who cannot be administered GBCA or during acute infarction. With dobutamine, viable myocardium will show improved contractility (including peri-infarct edematous tissue) negating the need for GBCA.

Nonischemic Cardiomyopathies

Hypertrophic cardiomyopathy

HCM is the most common inherited cardiac disorder with a prevalence of about 1:200 in the general population.[34,35] It has been defined as myocardial hypertrophy (more than or equal to 15 mm in the end-diastole) in the absence of after-load stresses that can explain the extent of hypertrophy, such as systemic hypertension, aortic coarctation, and aortic valve disease. Multiple studies over the past few years have established definite gene mutations responsible, including sarcomeric and

myofilament-related proteins.[36,37] Various phenotypic patterns of HCM are recognized: asymmetrical septal HCM, concentric and diffuse HCM, midventricular HCM, apical HCM, mass like HCM, burnt out HCM, genotype positive and phenotype negative HCM, etc., [Figure 6].[38]

CMR helps in confident diagnosis of HCM and also helps in exclusion of phenotypically similar conditions such as Anderson–Fabry disease and amyloidosis.[39] LV hypertrophy is the main feature of HCM found in MRI, apart from other typical findings including systolic anterior motion (SAM) of anterior mitral leaflet, high-normal or high ejection fraction and low indexed LV volumes. Supportive findings include dilated left atrium and mitral regurgitation. In addition, MRI can also depict certain genotypic markers to otherwise normal-appearing myocardium, such as papillary muscle anomalies, mitral valve anomalies, ventricular crypts, and hyper-trabeculated myocardium. LV cavity or outlet obstruction is an important feature (hypertrophic obstructive cardiomyopathy) and can be fixed (during systole and diastole) or dynamic (during systole). Obstruction is caused by thickened myocardium, papillary muscle abnormalities, SAM, or a combination of the above.

On LGE, areas of myocardial fibrosis are typically seen in the midmyocardium as patchy areas of enhancement. Enhancement can also be seen at RV insertion sites and at the subepicardial layer of the myocardium. Parametric mapping sequences are novel methods that help in the detection of fibrosis at an earlier stage than depicted by LGE sequences. Raised native T1, T2 and ECV values are the typical features [Figure 7].[40] T1 mapping also allows differentiation of HCM from other mimics such as Anderson–Fabry disease. Native T1 values of the myocardium are reduced in Anderson–Fabry compared to normal or raised values in HCM.[41] Advanced imaging techniques such as CMR diffusion tensor imaging and strain MRI are done to assess the myofibrillar orientation and LV function (regional and global) respectively.[42,43]

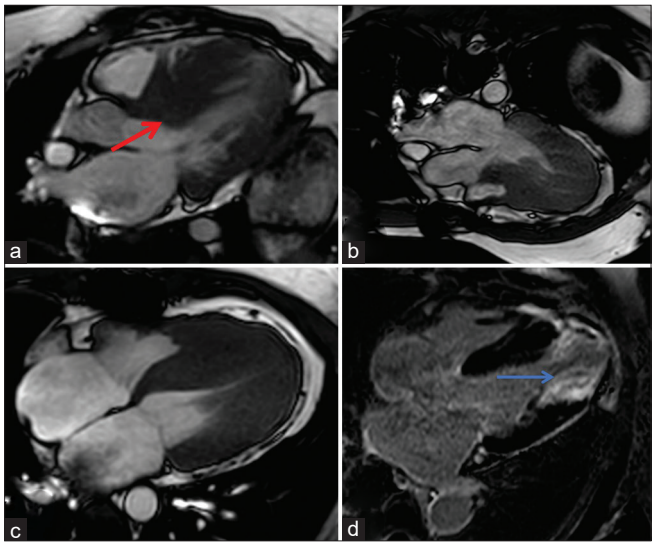

Figure 6: Hypertrophic Cardiomyopathy depiction by cardiac magnetic resonance. (a) Asymmetrical septal hyper trophy, primarily involving the basal septum (red arrow) (b) Symmetrical concentric variant of HCM. (c) Biventricular hypertrophic cardiomyopathy primarily involving the mid to apical cavity with obliteration of the apical cavity/apex. (d) Extensive fibrosis (blue arrow) in the apical cavity in late gadolinium enhancement images of a patient with apical variety of HCM. HCM: Hypertrophic cardiomyopathy

Poor prognostic indicators of HCM on CMR include: end-diastolic myocardial thickness of more than 30 mm, the fibrotic burden of more than 15%, RV involvement and LV outflow tract (LVOT) obstruction.[44-46]

Dilated cardiomyopathy

DCM is characterized by an increase in the LV end-diastolic diameters and/or volumes by more than 2 standard deviation along with a reduction in LV ejection fraction to <50%.[47] Numerous causes for DCM have been elucidated in the past, including idiopathic, ischemic, familial, infective, autoimmune, toxins, and metabolic pathologies.[48-50] Common genes associated with DCM include LMNA, TNNT2, BAG3 and RBM20.[50-53] DCM can also be broadly categorized into familial and nonfamilial forms.

CMR is being considered the best imaging modality for the evaluation of patients with DCM due to its ability to comprehensively assess cardiac anatomy, function and myocardial morphology together.[50] CMR plays a vital role in establishing the diagnosis, quantifying the ventricular function, demonstrating the etiology and highlighting the prognosis of patients with DCM. Serial CMR examinations are also helpful in accurately monitoring response to therapy.

Global or regional thinning of the myocardium along with poor systolic function are visualized and accurately quantified on cine CMR sequences. Myocardial edema is assessed using T2 weighted images (STIR/T2 maps) allowing diagnosis of acute myocardial inflammatory conditions. Differentiation of ischemic and nonischemic DCM is very important and can be easily achieved by CMR using stress perfusion imaging and LGE. Myocardial fibrosis in nonischemic DCM spares the subendocardium and typically involves the mid- or subepicardial myocardium. The fibrosis does not involve typical vascular territories in nonischemic DCM [Figure 8]. Furthermore, with CMR it is possible to assess extra cardiac structures which may help in establishing a diagnosis, for example, mediastinal lymphadenopathy in patients with cardiac sarcoidosis. LGE imaging may be normal in the early stages of DCM or in patients with diffuse myocardial fibrosis. Parametric mapping using native T1 and ECV is extremely helpful in this subgroup of patients. Phosphorus spectroscopy shows a reduction in phosphocreatine (PCr) with concomitant decrease in PCr/adenosine triphosphate ratio.[54]

Presence of fibrosis on LGE is associated with adverse cardiac prognosis, irrespective of the extent or pattern of fibrosis.[55] Midmyocardial enhancement especially along the septum is associated with a higher risk of significant cardiovascular events in the future in patients with nonischemic DCM.[56]

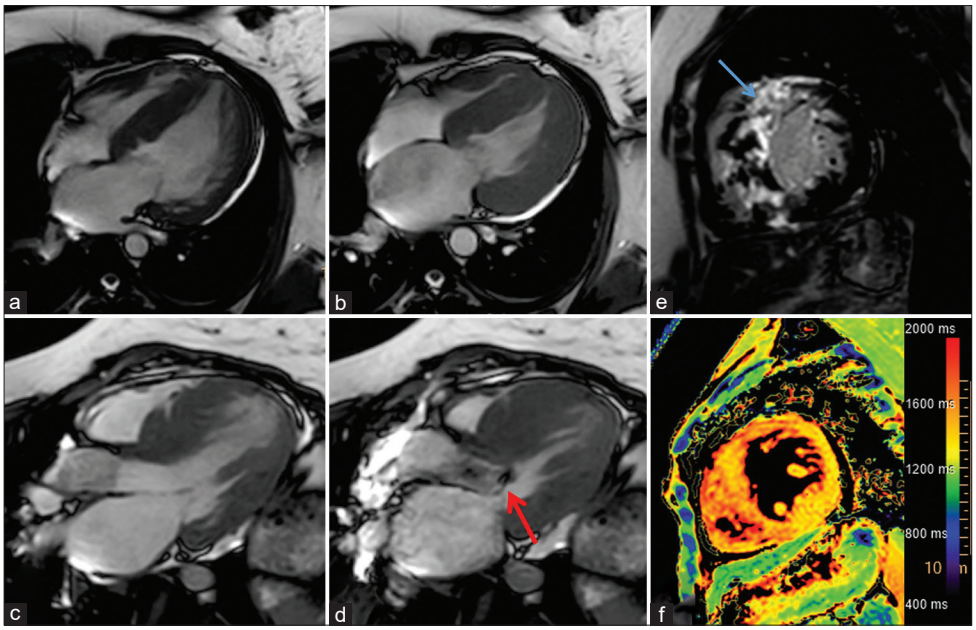

Figure 7: Comprehensive assessment of hypertrophic cardiomyopathy on cardiac magnetic resonance. Four-chamber steady-state-free-precession images in diastole (a) and systole (b) showing left ventricular hypertrophy without cavity obstruction. Three-chamber images in diastole (c) and systole (d) showing left ventricular outflow tract obstruction secondary to systolic anterior motion of mitral valve (red arrow) (e) Late gadolinium enhancement image showing midmyocardial enhancement predominantly along the septum (blue arrow) (f) Native T1 parametric map showing raised native T1 values

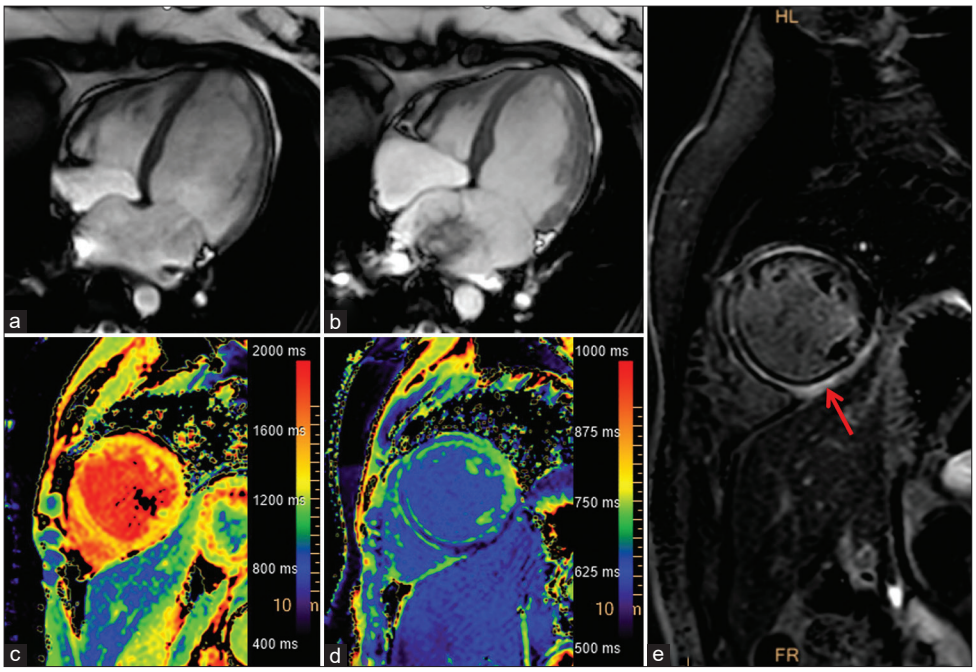

Figure 8: Nonischemic dilated cardiomyopathy. Four-chamber images in diastole (a) and systole (b) showing dilated ventricles with poor contraction. Native T1 parametric mapping (c) and extracellular volume (d) images showing raised values corresponding to areas of LGE. LGE image in short-axis (e) showing linear mid-myocardial enhancement along septum, anterior wall and epicardial enhancement along inferior wall (red arrow) in keeping with a nonischemic etiology. LGE: Late gadolinium enhancement

Arrhythmogenic right ventricular cardiomyopathy

Arrhythmogenic right ventricular cardiomyopathy (ARVC) is an autosomally dominant transmitted inheritable cardiomyopathy. It characteristically involves the RV, with varying amounts of LV involvement.[57] ARVC can lead to life-threatening ventricular arrhythmias, heart failure, and sudden cardiac death.[58] There have been recent changes to the diagnostic criteria of ARVC, which encompasses dominant right, biventricular, and dominant left arrhythmogenic cardiomyopathy (ACM).[59,60] CMR plays a pivotal role in the diagnosis of ACM by demonstrating

morphofunctional ventricular and structural myocardial abnormalities [Table 1]. The RV free wall is well visualized with CMR irrespective of the patient's body habitus. Axial cine images are preferred to view the RV compared to the short-axis images (better for LV). RV free wall akinesis, dyskinesis, or aneurysmal outpouchings are features seen in ARVC. It is also possible to see the "Accordion sign" (corrugations/striations along the RV free wall) and the presence of fat within the RV myocardium (this is however not part of the diagnostic criteria on CMR) [Figure 9]. Accurate quantification of ventricular volumes and demonstration of myocardial fibrosis are essential for the diagnosis of ACM as per the new criteria [Table 1].

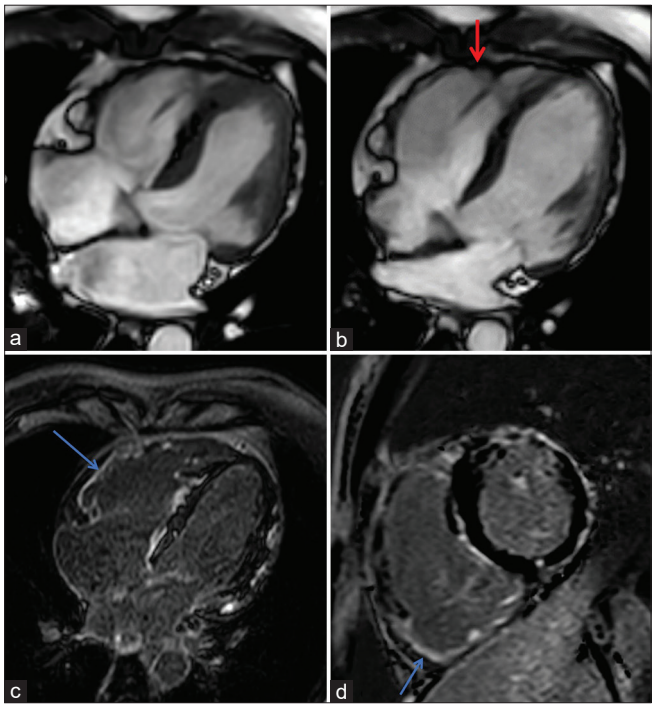

Figure 9: ARVC. Four chamber images in diastole (a) and systole (b) showing dyskinesia/early microaneurysms along the right ventricular free wall (red arrow). Late gadolinium enhancement images in four-chamber (c) and short-axis (d) planes showing the enhancement along the right ventricular free wall (blue arrow) and epicardial aspect of left ventricle in keeping with biventricular involvement of ARVC. ARVC: Arrhythmogenic right ventricular cardiomyopathy

A diagnosis of ARVC (dominant right variant of ACM) is met in patients fulfilling the RV criteria for "definite," i.e. 2 major or 1 major and 2 minor criteria or 4 minor criteria from different categories; "borderline," i.e. 1 major and 1 minor or 3 minor criteria from different categories; or "possible ARVC," i.e. 1 major or 2 minor criteria in the absence of LV involvement. The diagnosis of a "biventricular" variant requires one or more morphofunctional and/or structural abnormalities of both the right and left ventricles. The diagnosis of arrhythmogenic LV cardiomyopathy (Dominant-left variant) is met in patients who show structural abnormalities of LV, plus demonstration of an ACM-causing gene mutation, in the absence of RV involvement.

Restrictive cardiomyopathy

In restrictive cardiomyopathy, the myocardium is structurally and functionally abnormal.[61] It is characterized by restrictive ventricular physiology, which leads to diastolic dysfunction of the ventricles, while the systolic function is relatively well preserved in the early stages of the disease. Restrictive cardiomyopathy (RCM) is usually secondary to increased myocardial stiffness caused by various disorders including scleroderma, amyloidosis, sarcoidosis, glycogen storage disorders, iron overload, endomyocardial fibrosis, and certain drugs.[62]

Both functional assessment and routine morphological sequences are performed. Biatrial dilatation and demonstration of myocardial fibrosis/infiltration on LGE images help in the diagnosis [Figure 10]. Differentiation of one cause of RCM from the other is based on the pattern of LGE along with quantification of T1 and ECV. T1 values are classically raised in infiltrative diseases such as amyloidosis/sarcoidosis and reduced in some of the storage diseases such as Anderson–Fabry and iron deposition. T2* images also help in detection and quantification of myocardial iron content.[63]

Constrictive Pericarditis

This is a common indication for performing CMR. The role of imaging in these patients is to differentiate between constrictive pericarditis (CP) and restrictive cardiomyopathy, both of which have similar clinical features and impaired

Table 1: Magnetic resonance imaging criteria for diagnosis of arrhythmogenic right ventricular cardiomyopathy[60]

Category	Right ventricle (upgraded criteria)	Left ventricle (new criteria)
Morphofunctional ventricular abnormalities	Major Regional RV akinesia, dyskinesia or bulging plus one of the following Global RV dilatation (based on nomograms) Global RV systolic dysfunction (based on nomograms) Minor Regional RV akinesia, dyskinesia or aneurysm of RV free wall	Minor Global LV systolic dysfunction with or without LV dilatation Regional LV hypokinesia or akinesia of LV free wall, septum or both
Structural myocardial abnormalities	Major Transmural LGE of one or more RV regions (inlet, outlet and apex in 2 orthogonal views)	Major LV LGE of one or more bull's eye segments of the free wall (subepicardial or midmyocardial septum or both, excluding septal junction LGE)

LGE: Late gadolinium enhancement, LV: Left ventricular, RV: Right ventricular

ventricular filling. Often multimodality imaging is required to confidently differentiate these two entities as both have low or normal ventricular volumes, biatrial dilatation, impaired ventricular filling, and near-normal ventricular systolic function.[64]

In CMR, features of constrictive physiology include thickened and enhancing pericardium (>4 mm), interventricular septal bounce (with accentuation during Valsalva maneuver), ventricular deformation, and epicardial tethering.[65] STIR images can demonstrate pericardial edema in acute/subacute pericarditis [Figure 11].

Relative atrial volume ratio, defined as the ratio between volumes of the left and right atrium is seen to be significantly larger in patients with constrictive physiology than those with RCM.[64] Presence of pericardial edema and a higher quantitative pericardial LGE have a good prognosis in patients with CP.[66]

Unclassified Cardiomyopathies

Left ventricular noncompaction

LV noncompaction (LVNC) is characterized by the presence of excessive myocardial trabeculations with deep intertrabecular recesses that communicate with the ventricular cavity. This is secondary to the arrest of the normal maturation process of the myocardium.[67,68]

CMR aids in both phenotypic diagnosis and detection of co-existing congenital heart disorders. CMR can clearly differentiate the two layers of the myocardium (the thicker trabeculated/noncompacted endocardial layer and the thinner compacted/nontrabeculated epicardial layer).[69] The diagnostic criterion for LVNC on CMR is defined as the ratio of noncompact to compact myocardium being more than 2.3 [Figure 12]. The evaluation is done in the end-diastole phase in short-axis cine images. Quantification of myocardial mass with CMR is also useful in LVNC as trabeculated LV mass above 20% of the global LV mass is shown to be highly sensitive and specific for the diagnosis of LVNC.[70]

Parametric mapping in patients with LVNC shows increased native T1 and ECV values, with the native T1 changes being more prominent.[71] LGE images have varied appearances, including mid-myocardial and RV insertion site enhancement being the most commonly described. Other patterns less commonly seen include subendocardial and transmural enhancement.[72,73] Similar to speckle-tracking echocardiography, CMR strain analysis can demonstrate impaired global longitudinal strain and global circumferential strain.[74]

An important prognostic indicator is the extent of myocardial trabeculations, which can be assessed using multiple planes. The risk of major adverse cardiovascular and cerebrovascular events was high in patients with impaired LV function and in those with myocardial LGE. However, it was shown that noncompacted myocardial mass was not an independent predictor of major adverse events.[75,76]

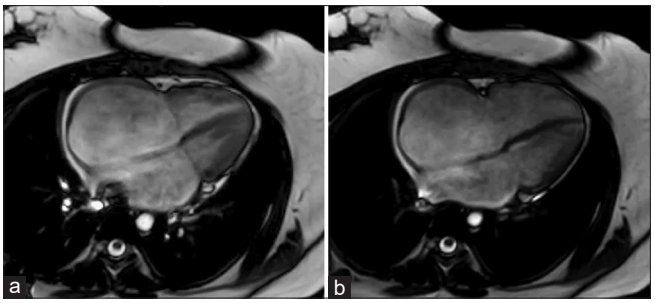

Figure 10: Four chamber steady-state-free-precession images in systole (a) and diastole (b) in a patient with restrictive cardiomyopathy showing biatrial enlargement

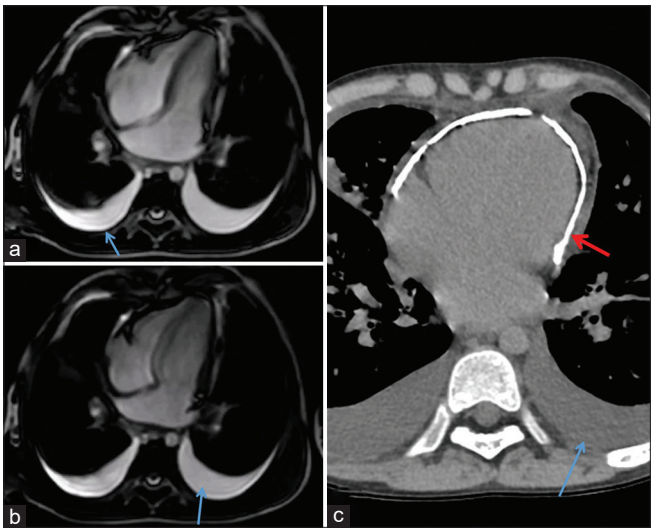

Figure 11: Constrictive pericarditis. Four-chamber image in diastole (a) and systole (b) showing elongated ventricles with extrinsic restriction to relation and dilated atria. (c) Computed tomography scan showing diffuse pericardial calcification (red arrow). Also seen are bilateral pleural effusions (blue arrows)

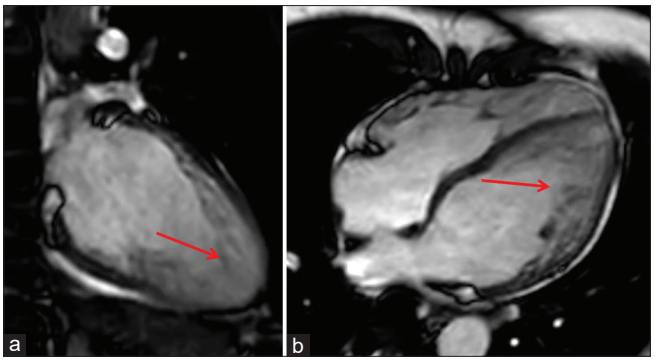

Figure 12: Left ventricular noncompaction. Two-chamber (a) and four-chamber (b) images in diastole showing the increased thickness of noncompacted myocardial layer (red arrows) compared to the peripheral compacted myocardium

Takotsubo cardiomyopathy

Takotsubo cardiomyopathy, also referred to as stress cardiomyopathy, gets its name from a Japanese "octopus pot" which has a narrow neck with a round bottom and is used to

trap octopuses.[77] It is characterized by acute and transient LV dysfunction (especially involving the apical segments) in the absence of obstructive coronary artery disease. Many patients are initially misdiagnosed with acute coronary syndrome due to the presence of chest pain with raised cardiac enzymes and accompanying electrocardiographic changes.[68] Various theories have been postulated, but a definitive pathology is yet to be identified. There are three major subtypes that have been described, including apical variant, mid-ventricular variant and basal variant (also called inverted Takotsubo) along with combinations of the above.[78]

CMR demonstrates wall motion abnormalities that tend to extend beyond a single coronary territory. It can also quantify ventricular function accurately and demonstrate the subtype of the disease. Mitral regurgitation is a common finding in cine magnetic resonance sequences, especially in those with apical and mid-ventricular variants.[79,80] Areas of myocardial edema are present and correspond to the regions of wall motion abnormalities.[81] LGE imaging is necessary to differentiate it from myocardial infarction and myocarditis where enhancement is almost always present, and lack of enhancement is a feature that is typical of Takotsubo cardiomyopathy.[82] Poor prognostic markers on CMR include involvement of right ventricle (biventricular pattern) and mid-ventricular subtype.[83,84]

Specific Cardiomyopathies

Iron overload cardiomyopathy

Myocardial iron overload can occur secondary to numerous causes including thalassemia, primary hemochromatosis, hepatic failure and multiple blood transfusions. CMR is highly accurate, sensitive and has high reproducibility in demonstration and quantification of myocardial iron overload.[85] Early detection is important so chelation therapy can be initiated to prevent the development of cardiomyopathy.[86] T2* imaging is the commonly used CMR sequence for this purpose. Iron has a tendency to reduce T1, T2, and T2* relaxation times by causing local magnetic field inhomogeneities leading to a signal drop on MRI. T1 mapping is also useful for the identification of iron overload (but not useful in quantification) and positive cases will have low myocardial native T1 value.[87] In T2*, sequential images of the heart and liver are taken while the patient is holding his/her breath. There is decay (reduction) in the signal from the tissue proportional to the degree of iron overload. With increased iron in the tissue, the signal decays faster (i.e. the tissue becomes darker) and this can be quantified. CMR based quantification of liver and myocardial iron overload has now made liver biopsies obsolete for iron quantification. Accurate quantification of LV function is also done in the same CMR sitting allowing a comprehensive assessment. A myocardial T2* of <10 ms is a poor prognostic feature and associated with LV dysfunction.[88]

Amyloidosis

Amyloidosis is characterized by the deposition of amyloid proteins in various tissues including the myocardium. Cardiac amyloidosis presents with restrictive physiology wherein the LV volumes and ejection fraction tend to be within normal limits in the early stages. LV wall thickness and myocardial mass are higher along with biatrial dilatation and often pericardial effusion at the time of presentation. LGE images are characteristic of cardiac amyloidosis and show a reversal of normal myocardial nulling pattern (seen in TI nulling sequences) due to extensive amyloid deposition within the myocardium. Circumferential subendocardial enhancement with some areas of transmural involvement is a classical pattern of LGE seen in cardiac amyloidosis [Figure 13]. Apical sparing can be seen in the majority of the patients with amyloidosis.[89] LGE imaging has also shown high accuracy in differentiation between different subtypes of amyloidosis.[90] T1 parametric mapping and ECV are revolutionizing the diagnosis, prognosis and follow-up of patients with amyloidosis. Both native T1 and ECV are raised in patients with amyloidosis and can be used as a marker to assess response to therapy. Based on pooled CMR data, various threshold values are being proposed for the diagnosis of amyloidosis by using native T1 mapping alone (negating the need of giving contrast). Native T1 is as good as LGE in prognosis of these patients and can be used for serial follow ups.[91]

Sarcoidosis

Sarcoidosis is a multisystem granulomatous disorder characterized on histopathology by noncaseating granulomas. Cardiac involvement in sarcoidosis is an important prognostic marker and can occur in up to 25% of patients with systemic sarcoidosis.[92] It is frequently underdiagnosed and can lead to significant morbidity and mortality. CMR can detect areas of active as well as chronic disease. During the acute inflammatory phase, focal areas of infiltration can be seen as T2 hyperintense (edema) with some wall thickening and wall motion abnormality on cine images. During chronic phase myocardial fibrosis can be seen in LGE with areas of thinning and scarring. LGE has become a modality of choice for assessment of these patients as it is associated with adverse events and cardiac death.[93] Enhancement is usually midmyocardial to epicardial in distribution and involves the septum, basal, and lateral segments of LV [Figure 14].[94] There is growing evidence supporting the use of CMR to assess for treatment response with steroids.[92,95] CMR findings can also be used to plan the site of endomyocardial biopsy for improved diagnostic yield. CMR also helps in concurrent assessment and follow up of mediastinal and hilar adenopathy in these patients.

Myocarditis

CMR is the most accurate and sensitive noninvasive imaging tool for evaluation of suspected myocarditis. CMR diagnosis of acute myocarditis is based on the Modified Lake Louise criteria (2018), which succeeded the original Lake Louise criteria (2009).[96,97] In the Modified Lake Louise criteria, both T1 based and T2 based imaging parameters are included and a component of both should be satisfied for a convincing diagnosis. There is improved detection of myocarditis on CMR using the new Lake Louise criteria.[98]

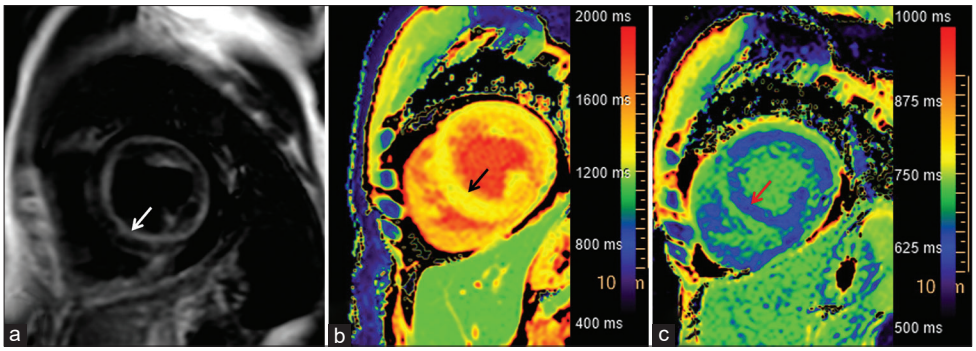

Figure 13: Cardiac amyloidosis. (a) Late gadolinium enhancement image in short-axis showing circumferential subendocardial enhancement (white arrow), (b) native T1 map showing diffusely raised T1 values (black arrow) and (c) raised myocardial extracellular volume (red arrow)

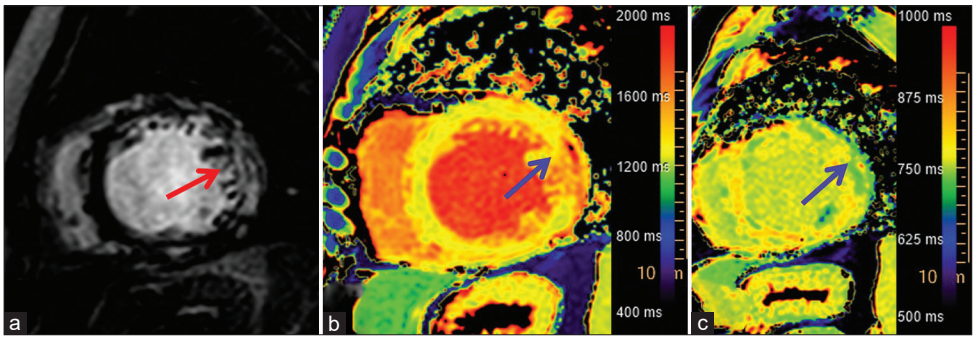

Figure 14: Late gadolinium enhancement image in short-axis (a) showing mid-myocardial to epicardial enhancement (red arrow) along the lateral wall with corresponding raised native T1 (b) and extracellular volume values (c) (blue arrows). This patient also had mediastinal lymph nodes which were biopsied and revealed sarcoid infiltration

T1 based imaging sequences include native myocardial T1 mapping, ECV and LGE imaging. An increase in native T1 relaxation times, increase in ECV or a positive nonischemic pattern of enhancement on LGE is needed to fulfill the criteria. The typical enhancement pattern includes subepicardial involvement in inferior and lateral segments and midwall involvement of the septum.

T2 based imaging sequences include T2 parametric mapping and STIR. An increase in T2 relaxation time or a regional high signal on STIR/high myocardial to skeletal muscle signal intensity ratio of ≥2 is essential. LGE in myocarditis is due to edema, and hence follow-up cases may show absence/reduction in the size of the enhancement [Figure 15].

Congenital/Structural Heart Diseases

CMR is a well-suited modality for the evaluation of CHD as it can provide both anatomical and functional information. In addition, it can also depict associated vascular abnormalities that may be overlooked on echocardiography. MRI can be used in the primary evaluation and in the postoperative follow-up of CHD. Owing to good spatial resolution, temporal resolution, multi-planar imaging capabilities, wide field of view and lack of ionizing radiation, CMR scores over other imaging modalities.[99] Accurate assessment of complex anatomy, myocardial tissue characterization, ventricular function, estimation of vessel flow and sizes can easily be done with CMR. Limitations include relatively longer scanning duration with the subject required to be less mobile, thus needing sedation, especially in neonates and smaller children.

Major applications of CMR in CHD include:

- Shunt quantification
- Quantification of differential pulmonary blood flow to right and left lung
- Accurate evaluation of ventricular volume and function (especially RV)
- Evaluation of valvular regurgitation
- Evaluation of associated vascular anomalies
- Evaluation of coexisting significant coronary artery disease in adults.[100]

Cardiac Tumors

Cardiac tumors can be primary, secondary or pseudotumors. CMR is an excellent modality for evaluation of these lesions. Echocardiography is generally the first investigative modality to detect these lesions as most are incidental in nature. Along with echocardiography, computed tomography can also provide limited morphological information, especially the presence of calcification. At times, a multimodality assessment is deemed necessary. Firstly, a cardiac tumor must be differentiated from a pseudotumor (such as thrombus). Further, the nature of the tumor is assessed.

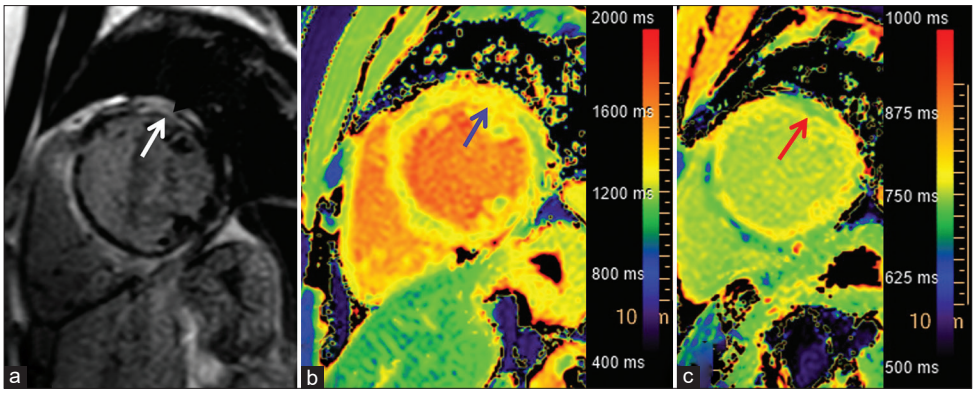

Figure 15: Myocarditis. (a) Late gadolinium enhancement image showing near circumferential epicardial enhancement with midmyocardial involvement along anterolateral segment (white arrow), (b) raised native T1, especially along the anterolateral segment (blue arrow) and (c) extracellular volume is correspondingly raised (red arrow)

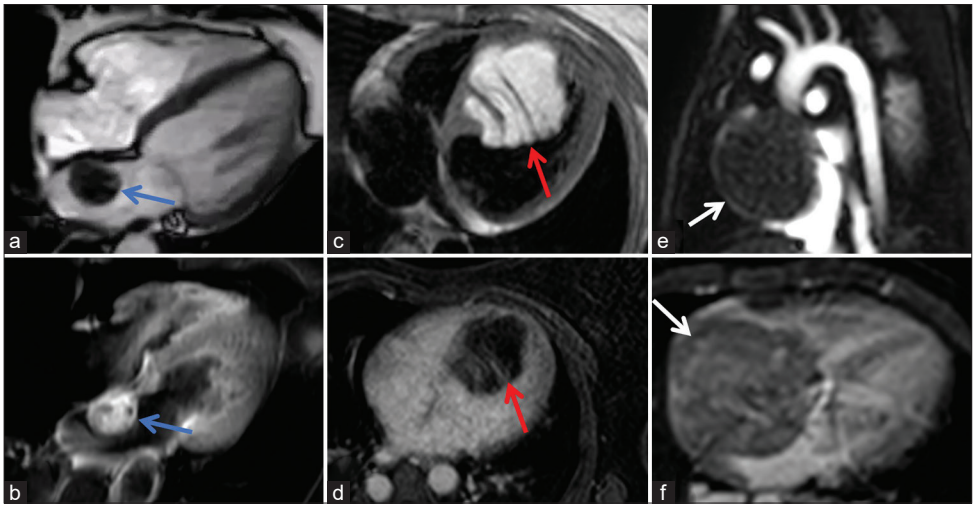

Figure 16: Cardiac masses. Cine 4-chamber (a) and short tau inversion recovery 4-chamber (b) images showing myxoma in left atrium attached to the interatrial septum (blue arrows). Axial T1 image (c) with lesion showing high signal in the interventricular septum with reversal of signal on T1 fat saturation (d) (red arrows) suggestive of lipoma. (e and f) Primary cardiac lymphoma- right atrial lesion attached predominantly to free wall with mild perfusion seen in short-axis perfusion image (e) with heterogeneous postcontrast enhancement (f) (white arrows)

CMR cine sequences can demonstrate the functional impact of intracardiac lesions such as LVOT obstruction or mitral valve obstruction. Characterization of cardiac tumors is best done on spin echo (SE) sequences and fat suppressed sequences (STIR). Contrast enhancement is another important feature to be assessed, which is done on both perfusion imaging and postcontrast T1 SE sequences. Signal intensities on SE sequences and assessment of vascularity on perfusion and postcontrast images provide sufficient information to characterize these lesions [Figure 16].

Conclusion

CMR is a great imaging modality for the evaluation of various myocardial pathology, owing to its excellent spatial resolution and ability to characterize myocardial morphology. When used appropriately, CMR helps in early diagnosis, accurate quantification, and prognostication of cardiomyopathies.

Acknowledgment

The authors would like to thank their entire team of nurses, technologists and other staff for their continued support and hard work in the Cardiothoracic Imaging Unit. We also would like to thank Dr Devi Prasad Shetty for his never-ending support and encouragement for academic work.

Financial support and sponsorship

Nil.

Conflicts of interest

There are no conflicts of interest.

References

1. Ortendahl D, Hylton N, Kaufman L. Tissue Characterization with MRI: The Value of the MR Parameters. In: Tissue Characterization in MR Imaging. 1st ed. Berlin, Heidelberg: Springer; 1990. p. 126-38.
2. Dandamudi S, Collins JD, Carr JC, Mongkolwat P, Rahsepar AA, Tomson TT, *et al.* The safety of cardiac and thoracic magnetic resonance

imaging in patients with cardiac implantable electronic devices. Acad Radiol 2016;23:1498-505.
3. Leong DP, De Pasquale CG, Selvanayagam JB. Heart failure with normal ejection fraction: The complementary roles of echocardiography and CMR imaging. JACC Cardiovasc Imaging 2010;3:409-20.
4. Simpson RM, Keegan J, Firmin DN. MR assessment of regional myocardial mechanics. J Magn Reson Imaging 2013;37:576-99.
5. Jeung MY, Germain P, Croisille P, El ghannudi S, Roy C, Gangi A. Myocardial tagging with MR imaging: Overview of normal and pathologic findings. Radiographics 2012;32:1381-98.
6. Petersen SE, Jung BA, Wiesmann F, Selvanayagam JB, Francis JM, Hennig J, *et al.* Myocardial tissue phase mapping with cine phase-contrast MR imaging: Regional wall motion analysis in healthy volunteers. Radiology 2006;238:816-26.
7. Neizel M, Lossnitzer D, Korosoglou G, Schäufele T, Lewien A, Steen H, *et al.* Strain-encoded (SENC) magnetic resonance imaging to evaluate regional heterogeneity of myocardial strain in healthy volunteers: Comparison with conventional tagging. J Magn Reson Imaging 2009;29:99-105.
8. Auger DA, Zhong X, Epstein FH, Spottiswoode BS. Mapping right ventricular myocardial mechanics using 3D cine DENSE cardiovascular magnetic resonance. J Cardiovasc Magn Reson 2012;14:4.
9. Youssef A, Ibrahim el-SH, Korosoglou G, Abraham MR, Weiss RG, Osman NF. Strain-encoding cardiovascular magnetic resonance for assessment of right-ventricular regional function. J Cardiovasc Magn Reson 2008;10:33.
10. Evin M, Cluzel P, Lamy J, Rosenbaum D, Kusmia S, Defrance C, *et al.* Assessment of left atrial function by MRI myocardial feature tracking. J Magn Reson Imaging 2015;42:379-89.
11. Dick A, Schmidt B, Michels G, Bunck AC, Maintz D, Baeßler B. Left and right atrial feature tracking in acute myocarditis: A feasibility study. Eur J Radiol 2017;89:72-80.
12. Biglands JD, Radjenovic A, Ridgway JP. Cardiovascular magnetic resonance physics for clinicians: Part II. J Cardiovasc Magn Reson 2012;14:66.
13. Haaf P, Garg P, Messroghli DR, Broadbent DA, Greenwood JP, Plein S. Cardiac T1 mapping and extracellular volume (ECV) in clinical practice: A comprehensive review. J Cardiovasc Magn Reson 2016;18:89.
14. Huelnhagen T, Paul K, Ku M, Serradas Duarte T, Niendorf T. Myocardial T2* mapping with ultrahigh field magnetic resonance: Physics and frontier applications. Front Phys 2017;5.1-19.
15. Sado DM, White SK, Piechnik SK, Banypersad SM, Treibel T, Captur G, *et al.* Identification and assessment of Anderson-Fabry disease by cardiovascular magnetic resonance noncontrast myocardial T1 mapping. Circ Cardiovasc Imaging 2013;6:392-8.
16. Andrew JT, Michael S, Rohan D, Michael JH. T1 Mapping: Basic techniques and clinical applications. J Am Coll Cardiol Imaging 2016;9:67-81.
17. Moon JC, Messroghli DR, Kellman P, Piechnik SK, Robson MD, Ugander M, *et al.* Myocardial T1 mapping and extracellular volume quantification: A society for cardiovascular magnetic resonance (SCMR) and CMR working group of the European society of cardiology consensus statement. J Cardiovasc Magn Reson 2013;15:92.
18. von Knobelsdorff-Brenkenhoff F, Prothmann M, Dieringer MA, Wassmuth R, Greiser A, Schwenke C, *et al.* Myocardial T1 and T2 mapping at 3 T: Reference values, influencing factors and implications. J Cardiovasc Magn Reson 2013;15:53.
19. Verhaert D, Thavendiranathan P, Giri S, Mihai G, Rajagopalan S, Simonetti OP, *et al.* Direct T2 quantification of myocardial edema in acute ischemic injury. JACC Cardiovasc Imaging 2011;4:269-78.
20. Wacker CM, Hartlep AW, Pfleger S, Schad LR, Ertl G, Bauer WR. Susceptibility-sensitive magnetic resonance imaging detects human myocardium supplied by a stenotic coronary artery without a contrast agent. J Am Coll Cardiol 2003;41:834-40.
21. Utz W, Jordan J, Niendorf T, Stoffels M, Luft FC, Dietz R, *et al.* Blood oxygen level-dependent MRI of tissue oxygenation: Relation to endothelium-dependent and endothelium-independent blood flow changes. Arterioscler Thromb Vasc Biol 2005;25:1408-13.
22. de Jong S, Zwanenburg JJ, Visser F, der Nagel Rv, van Rijen HV, Vos MA, *et al.* Direct detection of myocardial fibrosis by MRI. J Mol Cell Cardiol 2011;51:974-9.
23. ACR Committee on Drugs and Contrast Media. In: ACR Manual on Contrast Media. American College of Radiology; 2021. p. 85.
24. Weinreb JC, Rodby RA, Yee J, Wang CL, Fine D, McDonald RJ, *et al.* Use of intravenous gadolinium-based contrast media in patients with kidney disease: Consensus statements from the American college of radiology and the national kidney foundation. Kidney Med 2021;3:142-50.
25. Kramer CM, Barkhausen J, Flamm SD, Kim RJ, Nagel E, Society for Cardiovascular Magnetic Resonance Board of Trustees Task Force on Standardized Protocols. Standardized cardiovascular magnetic resonance imaging (CMR) protocols, society for cardiovascular magnetic resonance: Board of Trustees task force on standardized protocols. J Cardiovasc Magn Reson 2008;10:35.
26. Pozo E, Viliani D, Aguirre N, Agudo-Quilez P, Olivera MJ, Caballero P, *et al.* Early gadolinium enhancement in hypertrophic cardiomyopathy: A potential premature marker of myocardial damage. Int J Cardiovasc Imaging 2016;32:1635-43.
27. Raj V, Pudhiavan A, Hrishikesh VJ, Ali A, Kothari R. Safety profile of adenosine stress cardiac MRI in a tertiary hospital in India. Indian J Radiol Imaging 2020;30:459-64.
28. Charoenpanichkit C, Hundley WG. The 20 year evolution of dobutamine stress cardiovascular magnetic resonance. J Cardiovasc Magn Reson 2010;12:59.
29. Kuijpers D, Janssen CH, van Dijkman PR, Oudkerk M. Dobutamine stress MRI. Part I. Safety and feasibility of dobutamine cardiovascular magnetic resonance in patients suspected of myocardial ischemia. Eur Radiol 2004;14:1823-8.
30. Wahl A, Paetsch I, Gollesch A, Roethemeyer S, Foell D, Gebker R, *et al.* Safety and feasibility of high-dose dobutamine-atropine stress cardiovascular magnetic resonance for diagnosis of myocardial ischaemia: Experience in 1000 consecutive cases. Eur Heart J 2004;25:1230-6.
31. Ferrari V, Lombardi M, Plein S, Petersen S, Bucciarelli-Ducci C, Buechel E, *et al*. The EACVI Textbook of Cardiovascular Magnetic Resonance. 1st ed. Oxford: Oxford University Press; 2018.
32. Souto AL, Souto RM, Teixeira IC, Nacif MS. Myocardial viability on cardiac magnetic resonance. Arq Bras Cardiol 2017;108:458-69.
33. Baer FM, Theissen P, Schneider CA, Voth E, Sechtem U, Schicha H, *et al.* Dobutamine magnetic resonance imaging predicts contractile recovery of chronically dysfunctional myocardium after successful revascularization. J Am Coll Cardiol 1998;31:1040-8.
34. Wolf CM. Hypertrophic cardiomyopathy: Genetics and clinical perspectives. Cardiovasc Diagn Ther 2019;9:S388-415.
35. Semsarian C, Ingles J, Maron MS, Maron BJ. New perspectives on the prevalence of hypertrophic cardiomyopathy. J Am Coll Cardiol 2015;65:1249-54.
36. Maron BJ, Maron MS. Hypertrophic cardiomyopathy. Lancet 2013;381:242-55.
37. Seidman CE, Seidman JG. Identifying sarcomere gene mutations in hypertrophic cardiomyopathy: A personal history. Circ Res 2011;108:743-50.
38. Baxi AJ, Restrepo CS, Vargas D, Marmol-Velez A, Ocazionez D, Murillo H. Hypertrophic cardiomyopathy from A to Z: Genetics, pathophysiology, imaging, and management. Radiographics 2016;36:335-54.
39. Mavrogeni S, Markousis-Mavrogenis G, Markussis V, Kolovou G. The emerging role of cardiovascular magnetic resonance imaging in the evaluation of metabolic cardiomyopathies. Horm Metab Res 2015;47:623-32.
40. Huang L, Ran L, Zhao P, Tang D, Han R, Ai T, *et al*. MRI native T1 and T2 mapping of myocardial segments in hypertrophic cardiomyopathy: Tissue remodeling manifested prior to structure changes. Br J Radiol 2019;92:20190634. doi: 10.1259/bjr.20190634.
41. Radenkovic D, Weingärtner S, Ricketts L, Moon JC, Captur G. T_1 mapping in cardiac MRI. Heart Fail Rev 2017;22:415-30.
42. Ferreira PF, Kilner PJ, McGill LA, Nielles-Vallespin S, Scott AD, Ho SY, *et al. In vivo* cardiovascular magnetic resonance diffusion tensor imaging shows evidence of abnormal myocardial laminar orientations

and mobility in hypertrophic cardiomyopathy. J Cardiovasc Magn Reson 2014;16:87.
43. Haland TF, Almaas VM, Hasselberg NE, Saberniak J, Leren IS, Hopp E, *et al.* Strain echocardiography is related to fibrosis and ventricular arrhythmias in hypertrophic cardiomyopathy. Eur Heart J Cardiovasc Imaging 2016;17:613-21.
44. Brenes JC, Doltra A, Prat S. Cardiac magnetic resonance imaging in the evaluation of patients with hypertrophic cardiomyopathy. Glob Cardiol Sci Pract 2018;2018:22.
45. Mentias A, Raeisi-Giglou P, Smedira NG, Feng K, Sato K, Wazni O, *et al.* Late gadolinium enhancement in patients with hypertrophic cardiomyopathy and preserved systolic function. J Am Coll Cardiol 2018;72:857-70.
46. Keramida K, Lazaros G, Nihoyannopoulos P. Right ventricular involvement in hypertrophic cardiomyopathy: Patterns and implications. Hellenic J Cardiol 2020;61:3-8.
47. Pinto YM, Elliott PM, Arbustini E, Adler Y, Anastasakis A, Böhm M, *et al.* Proposal for a revised definition of dilated cardiomyopathy, hypokinetic non-dilated cardiomyopathy, and its implications for clinical practice: A position statement of the ESC working group on myocardial and pericardial diseases. Eur Heart J 2016;37:1850-8.
48. Hantson P. Mechanisms of toxic cardiomyopathy. Clin Toxicol (Phila) 2019;57:1-9.
49. O'Donnell DH, Abbara S, Chaithiraphan V, Yared K, Killeen RP, Martos R, *et al.* Cardiac MR imaging of nonischemic cardiomyopathies: Imaging protocols and spectra of appearances. Radiology 2012;262:403-22.
50. Schultheiss HP, Fairweather D, Caforio AL, Escher F, Hershberger RE, Lipshultz SE, *et al.* Dilated cardiomyopathy. Nat Rev Dis Primers 2019;5:32.
51. Brauch KM, Karst ML, Herron KJ, de Andrade M, Pellikka PA, Rodeheffer RJ, *et al.* Mutations in ribonucleic acid binding protein gene cause familial dilated cardiomyopathy. J Am Coll Cardiol 2009;54:930-41.
52. Norton N, Li D, Rieder MJ, Siegfried JD, Rampersaud E, Züchner S, *et al.* Genome-wide studies of copy number variation and exome sequencing identify rare variants in BAG3 as a cause of dilated cardiomyopathy. Am J Hum Genet 2011;88:273-82.
53. Kamisago M, Sharma SD, DePalma SR, Solomon S, Sharma P, McDonough B, *et al.* Mutations in sarcomere protein genes as a cause of dilated cardiomyopathy. N Engl J Med 2000;343:1688-96.
54. Francone M. Role of cardiac magnetic resonance in the evaluation of dilated cardiomyopathy: Diagnostic contribution and prognostic significance. ISRN Radiol 2014;2014:365404.
55. Wu KC, Weiss RG, Thiemann DR, Kitagawa K, Schmidt A, Dalal D, *et al.* Late gadolinium enhancement by cardiovascular magnetic resonance heralds an adverse prognosis in nonischemic cardiomyopathy. J Am Coll Cardiol 2008;51:2414-21.
56. Assomull RG, Prasad SK, Lyne J, Smith G, Burman ED, Khan M, *et al.* Cardiovascular magnetic resonance, fibrosis, and prognosis in dilated cardiomyopathy. J Am Coll Cardiol 2006;48:1977-85.
57. Calkins H, Corrado D, Marcus F. Risk stratification in arrhythmogenic right ventricular cardiomyopathy. Circulation 2017;136:2068-82.
58. Romero J, Mejia-Lopez E, Manrique C, Lucariello R. Arrhythmogenic right ventricular cardiomyopathy (ARVC/D): A systematic literature review. Clin Med Insights Cardiol 2013;7:97-114.
59. Marcus FI, McKenna WJ, Sherrill D, Basso C, Bauce B, Bluemke DA, *et al.* Diagnosis of arrhythmogenic right ventricular cardiomyopathy/dysplasia: Proposed modification of the task force criteria. Eur Heart J 2010;31:806-14.
60. Corrado D, Perazzolo Marra M, Zorzi A, Beffagna G, Cipriani A, Lazzari M, *et al.* Diagnosis of arrhythmogenic cardiomyopathy: The Padua criteria. Int J Cardiol 2020;319:106-14.
61. Elliott P, Andersson B, Arbustini E, Bilinska Z, Cecchi F, Charron P, *et al.* Classification of the cardiomyopathies: A position statement from the European society of cardiology working group on myocardial and pericardial diseases. Eur Heart J 2008;29:270-6.
62. Galea N, Polizzi G, Gatti M, Cundari G, Figuera M, Faletti R. Cardiovascular magnetic resonance (CMR) in restrictive cardiomyopathies. Radiol Med 2020;125:1072-86.
63. Anderson LJ, Holden S, Davis B, Prescott E, Charrier CC, Bunce NH, *et al.* Cardiovascular T2-star (T2*) magnetic resonance for the early diagnosis of myocardial iron overload. Eur Heart J 2001;22:2171-9.
64. Cheng H, Zhao S, Jiang S, Lu M, Yan C, Ling J, *et al.* The relative atrial volume ratio and late gadolinium enhancement provide additive information to differentiate constrictive pericarditis from restrictive cardiomyopathy. J Cardiovasc Magn Reson 2011;13:15.
65. Zurick AO, Bolen MA, Kwon DH, Tan CD, Popovic ZB, Rajeswaran J, *et al.* Pericardial delayed hyperenhancement with CMR imaging in patients with constrictive pericarditis undergoing surgical pericardiectomy: A case series with histopathological correlation. JACC Cardiovasc Imaging 2011;4:1180-91.
66. Alajaji W, Xu B, Sripariwuth A, Menon V, Kumar A, Schleicher M, *et al.* Noninvasive multimodality imaging for the diagnosis of constrictive pericarditis. Circ Cardiovasc Imaging 2018;11:e007878.
67. Zuccarino F, Vollmer I, Sanchez G, Navallas M, Pugliese F, Gayete A. Left ventricular noncompaction: Imaging findings and diagnostic criteria. AJR Am J Roentgenol 2015;204:W519-30.
68. O'Neill AC, McDermott S, Ridge CA, McDonald K, Keane D, Dodd JD. Uncharted waters: Rare and unclassified cardiomyopathies characterized on cardiac magnetic resonance imaging. Insights Imaging 2010;1:293-308.
69. Petersen SE, Selvanayagam JB, Wiesmann F, Robson MD, Francis JM, Anderson RH, *et al.* Left ventricular non-compaction: Insights from cardiovascular magnetic resonance imaging. J Am Coll Cardiol 2005;46:101-5.
70. Jacquier A, Thuny F, Jop B, Giorgi R, Cohen F, Gaubert JY, *et al.* Measurement of trabeculated left ventricular mass using cardiac magnetic resonance imaging in the diagnosis of left ventricular non-compaction. Eur Heart J 2010;31:1098-104.
71. Araujo-Filho JA, Assuncao AN Jr., Tavares de Melo MD, Bière L, Lima CR, Dantas RN Jr., *et al.* Myocardial T1 mapping and extracellular volume quantification in patients with left ventricular non-compaction cardiomyopathy. Eur Heart J Cardiovasc Imaging 2018;19:888-95.
72. Wan J, Zhao S, Cheng H, Lu M, Jiang S, Yin G, *et al.* Varied distributions of late gadolinium enhancement found among patients meeting cardiovascular magnetic resonance criteria for isolated left ventricular non-compaction. J Cardiovasc Magn Reson 2013;15:20.
73. Nucifora G, Aquaro GD, Pingitore A, Masci PG, Lombardi M. Myocardial fibrosis in isolated left ventricular non-compaction and its relation to disease severity. Eur J Heart Fail 2011;13:170-6.
74. Gastl M, Gotschy A, Polacin M, Vishnevskiy V, Meyer D, Sokolska J, *et al.* Determinants of myocardial function characterized by CMR-derived strain parameters in left ventricular non-compaction cardiomyopathy. Sci Rep 2019;9:15882.
75. Femia G, Zhu D, Choudhary P, Ross SB, Muthurangu V, Richmond D, *et al.* Long term clinical outcomes associated with CMR quantified isolated left ventricular non-compaction in adults. Int J Cardiol 2021;328:235-40.
76. Grigoratos C, Barison A, Ivanov A, Andreini D, Amzulescu MS, Mazurkiewicz L, *et al.* Meta-analysis of the prognostic role of late gadolinium enhancement and global systolic impairment in left ventricular noncompaction. JACC Cardiovasc Imaging 2019;12:2141-51.
77. Dote K, Sato H, Tateishi H, Uchida T, Ishihara M. Myocardial stunning due to simultaneous multivessel coronary spasms: A review of 5 cases. J Cardiol 1991;21:203-14.
78. Abraham J, Mudd JO, Kapur NK, Klein K, Champion HC, Wittstein IS. Stress cardiomyopathy after intravenous administration of catecholamines and beta-receptor agonists. J Am Coll Cardiol 2009;53:1320-5.
79. Song BG, Chun WJ, Park YH, Kang GH, Oh J, Lee SC, *et al.* The clinical characteristics, laboratory parameters, electrocardiographic, and echocardiographic findings of reverse or inverted takotsubo cardiomyopathy: Comparison with mid or apical variant. Clin Cardiol 2011;34:693-9.
80. Kohan AA, Levy Yeyati E, De Stefano L, Dragonetti L, Pietrani M, Perez de Arenaza D, *et al.* Usefulness of MRI in takotsubo cardiomyopathy: A review of the literature. Cardiovasc Diagn Ther 2014;4:138-46.

81. Eitel I, von Knobelsdorff-Brenkenhoff F, Bernhardt P, Carbone I, Muellerleile K, Aldrovandi A, *et al.* Clinical characteristics and cardiovascular magnetic resonance findings in stress (takotsubo) cardiomyopathy. JAMA 2011;306:277-86.
82. Eitel I, Behrendt F, Schindler K, Kivelitz D, Gutberlet M, Schuler G, *et al.* Differential diagnosis of suspected apical ballooning syndrome using contrast-enhanced magnetic resonance imaging. Eur Heart J 2008;29:2651-9.
83. Stiermaier T, Santoro F, Eitel C, Graf T, Möller C, Tarantino N, *et al.* Prevalence and prognostic relevance of atrial fibrillation in patients with takotsubo syndrome. Int J Cardiol 2017;245:156-61.
84. Lyon AR, Bossone E, Schneider B, Sechtem U, Citro R, Underwood SR, *et al.* Current state of knowledge on takotsubo syndrome: A position statement from the taskforce on takotsubo syndrome of the heart failure association of the European society of cardiology. Eur J Heart Fail 2016;18:8-27.
85. Anderson LJ. Assessment of iron overload with T2* magnetic resonance imaging. Prog Cardiovasc Dis 2011;54:287-94.
86. Tanner MA, Galanello R, Dessi C, Smith GC, Westwood MA, Agus A, *et al.* Combined chelation therapy in thalassemia major for the treatment of severe myocardial siderosis with left ventricular dysfunction. J Cardiovasc Magn Reson 2008;10:12.
87. Meloni A, Martini N, Positano V, De Luca A, Pistoia L, Sbragi S, *et al.* Myocardial iron overload by cardiovascular magnetic resonance native segmental T1 mapping: A sensitive approach that correlates with cardiac complications. J Cardiovasc Magn Reson 2021;23:70.
88. Ngim CF, Lee MY, Othman N, Lim SM, Ng CS, Ramadas A. Prevalence and risk factors for cardiac and liver iron overload in adults with thalassemia in malaysia. Hemoglobin 2019;43:95-100.
89. Balzer P, Furber A, Delépine S, Rouleau F, Lethimonnier F, Morel O, *et al.* Regional assessment of wall curvature and wall stress in left ventricle with magnetic resonance imaging. Am J Physiol 1999;277:H901-10.
90. Dungu JN, Valencia O, Pinney JH, Gibbs SD, Rowczenio D, Gilbertson JA, *et al.* CMR-based differentiation of AL and ATTR cardiac amyloidosis. JACC Cardiovasc Imaging 2014;7:133-42.
91. Pan JA, Kerwin MJ, Salerno M. Native T1 mapping, extracellular volume mapping, and late gadolinium enhancement in cardiac amyloidosis: A meta-analysis. JACC Cardiovasc Imaging 2020;13:1299-310.
92. Perez IE, Garcia MJ, Taub CC. Multimodality imaging in cardiac sarcoidosis: Is there a winner? Curr Cardiol Rev 2016;12:3-11.
93. Greulich S, Deluigi CC, Gloekler S, Wahl A, Zürn C, Kramer U, *et al.* CMR imaging predicts death and other adverse events in suspected cardiac sarcoidosis. JACC Cardiovasc Imaging 2013;6:501-11.
94. Smedema JP, Snoep G, van Kroonenburgh MP, van Geuns RJ, Dassen WR, Gorgels AP, *et al.* Evaluation of the accuracy of gadolinium-enhanced cardiovascular magnetic resonance in the diagnosis of cardiac sarcoidosis. J Am Coll Cardiol 2005;45:1683-90.
95. Shimada T, Shimada K, Sakane T, Ochiai K, Tsukihashi H, Fukui M, *et al.* Diagnosis of cardiac sarcoidosis and evaluation of the effects of steroid therapy by gadolinium-DTPA-enhanced magnetic resonance imaging. Am J Med 2001;110:520-7.
96. Friedrich MG, Sechtem U, Schulz-Menger J, Holmvang G, Alakija P, Cooper LT, *et al.* Cardiovascular magnetic resonance in myocarditis: A JACC White Paper. J Am Coll Cardiol 2009;53:1475-87.
97. Ferreira VM, Schulz-Menger J, Holmvang G, Kramer CM, Carbone I, Sechtem U, *et al.* Cardiovascular magnetic resonance in nonischemic myocardial inflammation: Expert recommendations. J Am Coll Cardiol 2018;72:3158-76.
98. Cundari G, Galea N, De Rubeis G, Frustaci A, Cilia F, Mancuso G, *et al.* Use of the new Lake Louise Criteria improves CMR detection of atypical forms of acute myocarditis. Int J Cardiovasc Imaging 2021;37:1395-404.
99. Rajiah P, Tandon A, Greil GF, Abbara S. Update on the role of cardiac magnetic resonance imaging in congenital heart disease. Curr Treat Options Cardiovasc Med 2017;19:2.
100. Baumgartner H, De Backer J, Babu-Narayan SV, Budts W, Chessa M, Diller GP, *et al.* 2020 ESC Guidelines for the management of adult congenital heart disease. Eur Heart J 2021;42:563-645.